Gaucher Disease Glucocerebrosidase and α-Synuclein Form a Bidirectional Pathogenic Loop in Synucleinopathies

Joseph R. Mazzulli,[1] You-Hai Xu,[2,3] Ying Sun,[2,3] Adam L. Knight,[4] Pamela J. McLean,[1] Guy A. Caldwell,[4,5] Ellen Sidransky,[6] Gregory A. Grabowski,[2,3] and Dimitri Krainc[1,*]

[1]Department of Neurology, Massachusetts General Hospital, Harvard Medical School, MassGeneral Institute for Neurodegenerative Disease, Charlestown, MA 02129, USA
[2]The Division of Human Genetics, Cincinnati Children's Hospital Medical Center, Cincinnati, OH 45229, USA
[3]Department of Pediatrics, University of Cincinnati College of Medicine, Cincinnati, OH 45229, USA
[4]Department of Biological Sciences, University of Alabama, Tuscaloosa, AL 35487, USA
[5]Departments of Neurology and Neurobiology, Center for Neurodegeneration and Experimental Therapeutics, University of Alabama at Birmingham, Birmingham, AL 35294, USA
[6]Section on Molecular Neurogenetics, Medical Genetics Branch, National Human Genome Research Institute, National Institutes of Health, Bethesda, MD 20892, USA
*Correspondence: krainc@mgh.helix.harvard.edu

SUMMARY

Parkinson's disease (PD), an adult neurodegenerative disorder, has been clinically linked to the lysosomal storage disorder Gaucher disease (GD), but the mechanistic connection is not known. Here, we show that functional loss of GD-linked glucocerebrosidase (GCase) in primary cultures or human iPS neurons compromises lysosomal protein degradation, causes accumulation of α-synuclein (α-syn), and results in neurotoxicity through aggregation-dependent mechanisms. Glucosylceramide (GlcCer), the GCase substrate, directly influenced amyloid formation of purified α-syn by stabilizing soluble oligomeric intermediates. We further demonstrate that α-syn inhibits the lysosomal activity of normal GCase in neurons and idiopathic PD brain, suggesting that GCase depletion contributes to the pathogenesis of sporadic synucleinopathies. These findings suggest that the bidirectional effect of α-syn and GCase forms a positive feedback loop that may lead to a self-propagating disease. Therefore, improved targeting of GCase to lysosomes may represent a specific therapeutic approach for PD and other synucleinopathies.

INTRODUCTION

The synucleinopathies, including dementia with Lewy bodies (DLB) and Parkinson's disease (PD), are a group of neurodegenerative disorders characterized by the accumulation of α-syn, a small neural-specific protein involved in synaptic function (Chandra et al., 2005). Although clinically diverse, the synuclei-nopathies are all characterized by the presence of aggregated, insoluble α-syn within Lewy bodies and Lewy neurites of the central nervous system in the form of typical amyloid fibrils (Trojanowski and Lee, 2002). The identification of PD-causing mutations in α-syn, which accelerate aggregation in vitro (Conway et al., 1998) and in transgenic mice (Chandra et al., 2005; Giasson et al., 2002), indicates that the formation of fibrils is an important pathogenic event. Recent evidence using in vitro systems has also indicated that soluble oligomeric α-syn assemblies, intermediates in fibril formation, can be cytotoxic (Kayed et al., 2003; Volles and Lansbury, 2003). However, the documentation and characterization of these species in vivo have been hampered by technical limitations as well as their evanescent nature in cells. Further, the in vivo factors that dictate the formation and stabilization of these putatively toxic intermediates are not known.

Recent description of a clinical link between GD and parkinsonism (Sidransky, 2005) suggested that mutations in the GCase gene (*GBA1)* and alterations in sphingolipid metabolism contribute to the pathogenesis of synucleinopathies. GD is a rare, autosomal recessive lysosomal storage disorder that results from loss-of-function mutations in GCase, a lysosomal enzyme that cleaves the β-glucosyl linkage of GlcCer (Brady et al., 1965). Three types of GD have been described, based on the rate of clinical progression and involvement of the nervous system (Grabowski, 2008). Type I GD is classically defined as non-neuronopathic and is typically characterized by hepatosplenomegaly, skeletal and hematopoietic system abnormalities. Phenotypic variation in type I GD has been observed, and a small subset of patients develop parkinsonism at variable ages throughout the course of the disease (Bultron et al., 2010; Tayebi et al., 2003). Types II and III are differentiated from type I by neurodegeneration of the central nervous system with either rapid (type II) or chronic progression (type III); however these forms can also show some phenotypic variation. A common feature of all three types is accumulation of GlcCer in the affected

tissues, but the reasons for phenotypic variability of GD are not known.

The initial discovery of parkinsonism in a subset of adult onset type I GD patients suggested a possible pathogenic link between the two disorders (Neudorfer et al., 1996; Sidransky, 2005; Tayebi et al., 2003). Neuropathological analysis of these patients revealed the presence of α-syn-positive Lewy bodies (Wong et al., 2004), suggesting the involvement of α-syn aggregation. It was subsequently noted that patients with GD and parkinsonism frequently had relatives with parkinsonism that were heterozygous for *GBA1* mutations (Goker-Alpan et al., 2004). Importantly, several additional genetic studies in large patient cohorts demonstrated that patients with parkinsonism have an increased incidence of *GBA1* mutations (Lill et al., 2008; Sidransky et al., 2009), making *GBA1* the most common known genetic risk factor for PD to date. *GBA1* mutations have also been identified in patients with the diagnosis of DLB (Goker-Alpan et al., 2006; Neumann et al., 2009), and inhibitors of GCase function have been shown to modulate α-syn levels (Manning-Bog et al., 2009). While these studies provide correlative evidence in patients that GlcCer metabolism may be linked to α-syn, the mechanism of such linkage has not been explored. Here, we show that intracellular GlcCer levels control the formation of soluble toxic α-syn assemblies in cultured neurons and mouse and human brain, leading to neurodegeneration. The elevation and formation of α-syn assemblies further contributes to a pathogenic cycle by inhibiting the lysosomal maturation and activity of normal GCase, resulting in additional GlcCer accumulation and augmented α-syn oligomer formation.

RESULTS

Depletion of GCase Compromises Protein Degradation Capacity and Increases α-Syn Levels in Neurons

The observation that loss-of-function GCase mutations cause α-syn accumulation and Lewy bodies in GD brain prompted us to test the biological effects of GCase knockdown (KD) in neurons. GCase shRNA-mediated KD by lentiviral infection resulted in a 50% reduction in GCase protein levels compared to nontransduced neurons control scrambled (scrb) shRNA-infected neurons (Figures 1A and 1B). The levels of mature lysosomal GCase were analyzed by endoglycosidase H (endo H) treatment, an enzyme that only cleaves high mannose moieties of endoplasmic reticulum (ER) proteins. This revealed lower levels of endo H-resistant GCase upon infection with GCase shRNA constructs, demonstrating a depletion of the lysosomal form (Figure S1A available online). Further analysis of whole-cell lysates showed a decline in GCase activity (Figure 1B), increased cellular lipids with BODIPY 493, and increased GlcCer by immunofluorescence (Figures 1C and 1D). GlcCer accumulation was validated by mass spectrometry, which revealed a 4-fold increase of GlcCer in GCase-depleted neurons, whereas the levels of ceramide and other sphingolipids remained unchanged (Figure 1B, Figure S1D). Analysis of other lysosomal proteins and activity suggested that the constructs specifically decrease GCase protein (Figures S1C–S1F). Neurotoxicity was assessed upon GCase KD by neurofilament (NF) immunostaining, a sensitive method that detects the degeneration of neurites

in cell culture before the occurrence of more severe nuclear toxicity (Zala et al., 2005). This revealed no change in neurotoxicity when assessed at 7 days post-infection (dpi), suggesting that neurons have the ability to tolerate alterations in the GlcCer metabolizing pathway within this timeframe.

We next analyzed proteolysis of long-lived proteins in living neurons and found that GCase KD significantly decreased the rate of proteolysis by 40% (Figure 1E, Figure S1B). To determine whether GCase KD affects a lysosomal degradation pathway, neurons were treated with the well-established lysosomal inhibitors ammonium chloride (NH_4Cl) and leupeptin. These compounds did not additively inhibit the proteolysis in GCase shRNA-treated cells, indicating that GCase KD affects a lysosomal-mediated pathway (Figure 1E). Consistent with this, immunofluorescence analysis of LAMP1, a lysosomal marker, revealed accumulation and enlargement of LAMP1-positive puncta in neurons (Figure S1G).

Because Lewy bodies have been detected in postmortem brain samples of patients with GD, we hypothesized that endogenous α-syn protein may accumulate in neurons infected with GCase shRNA. Indeed, GCase KD increased the steady-state levels of α-syn by 1.8-fold relative to controls, whereas the levels of another disease-associated aggregation-prone protein, tau, did not change (Figure 1F). This also occurred without a change in mRNA levels of α-syn, suggesting that the observed increase in α-syn protein levels resulted from compromised protein degradation (Figure 1F). Analysis of α-syn levels after GCase KD was also performed in a human neuroglioma cell line (H4) expressing wild-type (WT) α-syn under the control of a tetracycline-inducible promoter ("tet-off"). α-syn expression was turned off by dox to determine the α-syn degradation rate. This revealed that GCase KD impeded the clearance of α-syn (Figure 1G). Taken together, these data suggest that KD of GCase in neurons leads to decreased lysosomal degradation capacity and consequently increased levels of α-syn protein.

To validate the primary culture results, dopaminergic neurons were generated from induced pluripotent stem (iPS) cells derived from skin fibroblasts of a GD patient. Analysis of GD iPS cells revealed the expression of Oct4, Tra-1-60, SSEA-4, and nanog, indicating that GD iPS cells contain the essential pluripotency factors, as well as normal chromosomal number, size, and genomic structure (Figures S2A and S2B). Dopaminergic neurons were induced from iPS cells by a previously established protocol (Seibler et al., 2011) to yield ∼80% of cells that expressed the neuron-specific β III tubulin, and ∼10% that expressed the dopaminergic marker tyrosine hydroxylase (TH) (Figure 2A). Genotyping analysis confirmed that GD, but not WT, iPS neurons harbored the expected mutations in GCase (N370S/84GG insertion) and lower levels of GCase protein and activity (Figure 2B, Table S1). In addition, WT and GD cells did not contain other mutations previously shown to cause PD (Table S1). Radioactive pulse-chase experiments in GD iPS neurons revealed a decline in proteolysis of long-lived proteins compared to WT cells, and the addition of lysosomal inhibitors did not further affect proteolysis (Figure 2C). Proteolysis measurement of short-lived proteins revealed no change compared to WT cells (Figure 2C, inset). Immunofluoresence and western blot analysis revealed a dramatic increase in α-syn protein levels in GD iPS
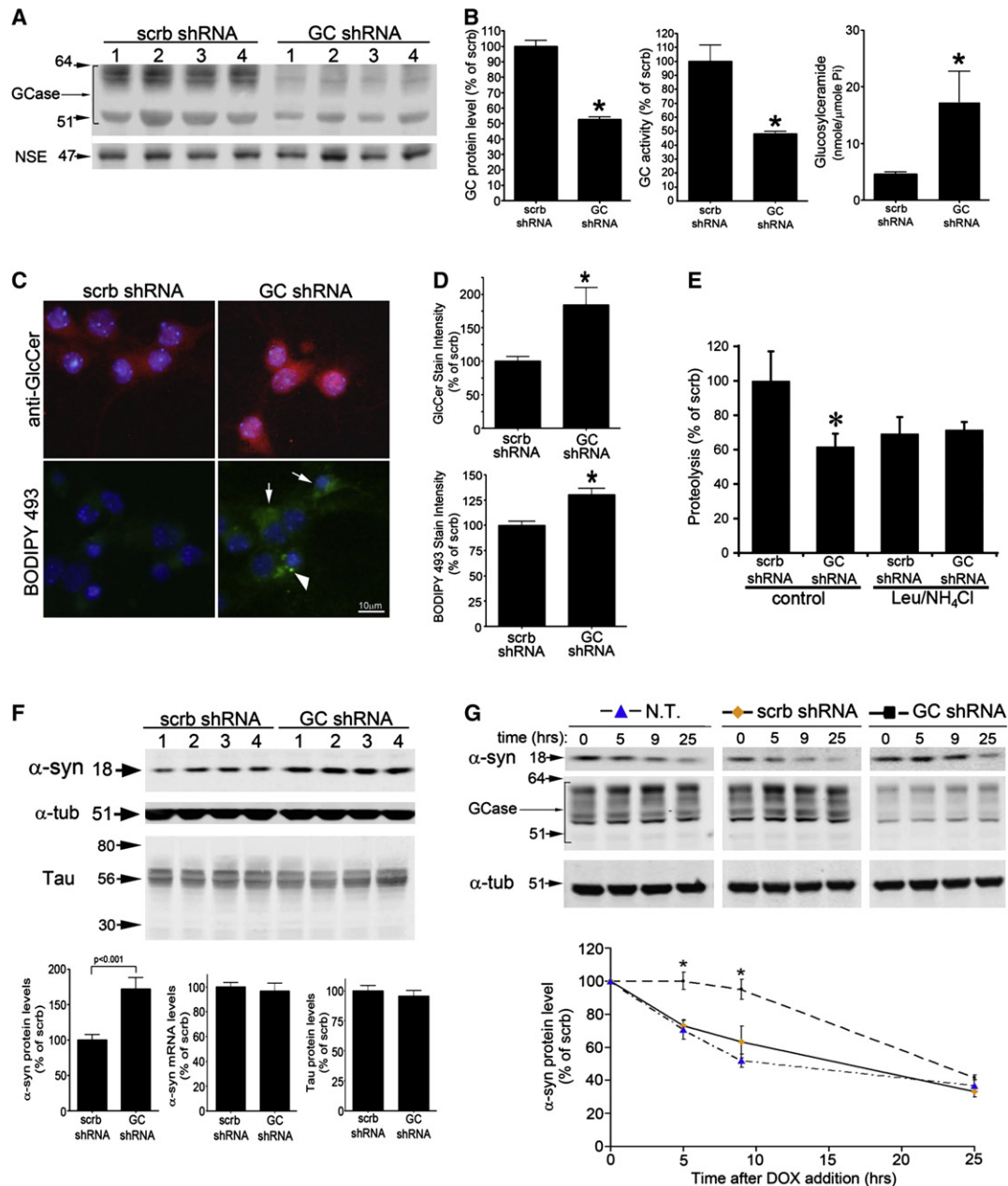
Figure 1. GCase Knockdown Compromises Lysosomal Degradation and Causes Accumulation of α-Syn

(A) KD of GCase protein in cortical neurons by GCase shRNA is shown by western blot. Neural specific enolase (NSE) was used as a loading control. Four replicates are shown. Scrb, scrambled shRNA.

(B) Left: GCase protein levels (n = 6, *p < 0.01). Middle: Enzymatic activity of GCase (n = 6, *p < 0.01). Right: Intracellular GlcCer quantification by MS (Pi, phosphate) (n = 3, *p < 0.05).

(C) GlcCer immunofluorescence (top, red) and neutral lipids were visualized by BODIPY 493 fluorescence (bottom, green). Nuclei were visualized with DAPI (blue). The arrows indicate cells with increased diffuse staining, whereas the arrowhead indicates a cell with punctated lipid accumulations.

(D) Fluorescent intensity shown in (C) was quantified and normalized to DAPI (n = 3, *p < 0.05).

(E) Proteolysis of long-lived proteins in neurons assessed at 8 hr. Lysosomal inhibitors leupeptin (leu) and ammonium chloride (NH_4Cl) were used (n = 4, *p < 0.05).

(F) Western blot of endogenous α-syn (mAb syn202) and Tau. Four replicates are shown. Protein and mRNA levels are shown under the blots (n = 4, *p < 0.05). α-Tub was used as a loading control.

(G) α-Syn analysis in inducible H4 cells. Expression was turned off by doxycycline (DOX) and protein clearance was measured by western blot with mAb syn211. Quantifications are shown below (n = 6, *p < 0.05). GCase KD is shown by western blot and α-tub was used as a loading control. Molecular weight (MW) is indicated in kDa. For all analyses, values are the mean ± standard error of the mean (SEM).

See also Figure S1.
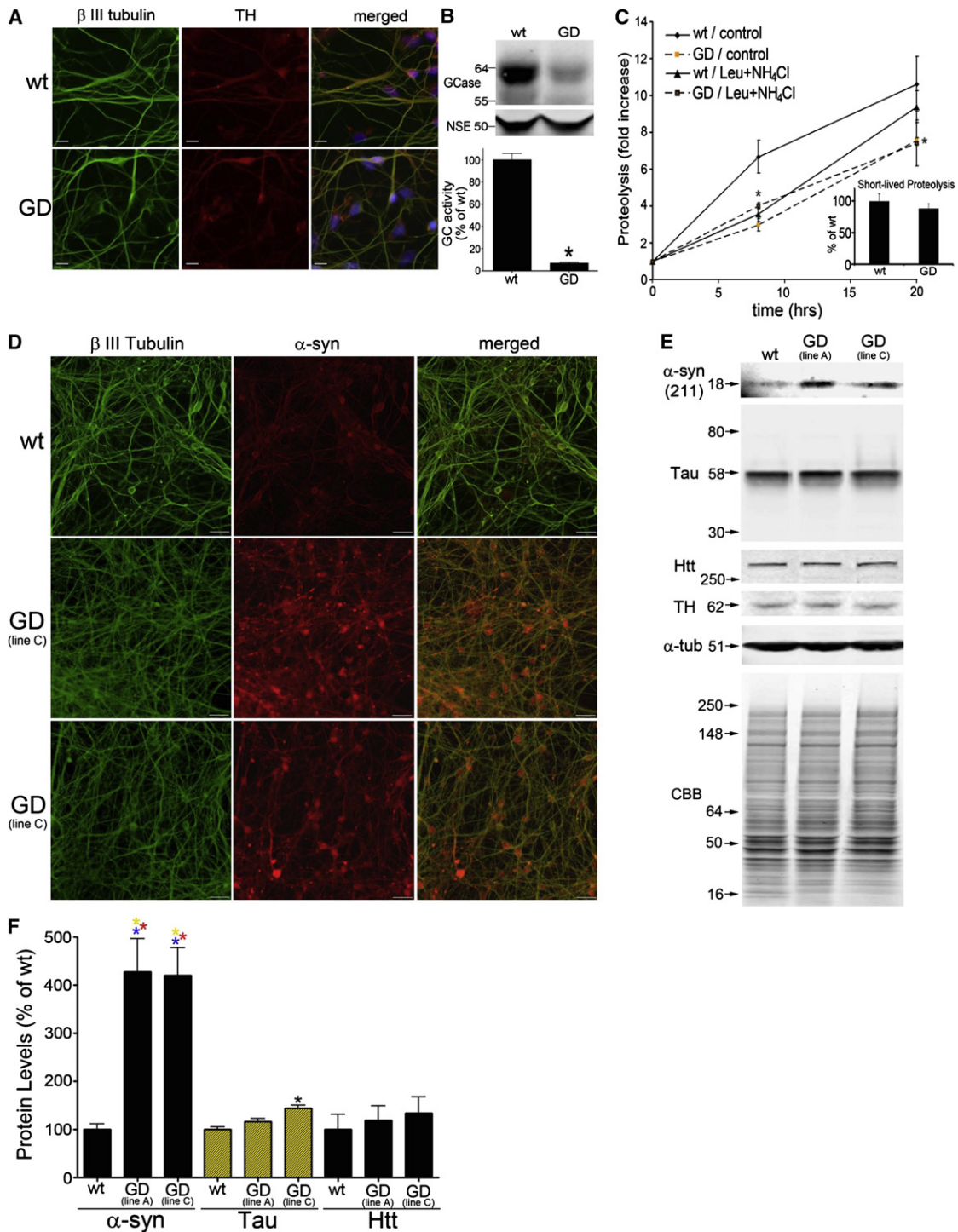
Figure 2. Compromised Proteolysis of Long-Lived Proteins and Specific Accumulation of Endogenous α-Syn in Human GD Dopaminergic Neurons

(A) Immunofluorescence analysis of WT and GD neurons generated from iPS cells with the neuronal marker β III tubulin (green) and catecholaminergic marker tyrosine hydroxylase (TH, red). Nuclei (DAPI) are shown in blue. Scale bars = 10 μm.

(B) Western blot analysis of GCase. NSE was used as a loading control. Bottom, quantification of GCase activity (n = 3, *p < 0.05).

(C) Long-lived protein degradation was assessed as in Figure 1E (n = 4, *p < 0.05). Inset, proteolysis of short-lived proteins (15 min post-chase).

(D) α-Syn immunofluorescence analysis using mAb LB509 (red). β III tubulin, green. Scale bar = 30 μm.

(E) Western blot of T-sol lysates from iPS neurons. Htt, huntingtin; CBB, Coomassie brilliant blue.

neurons compared to WT cells (Figures 2D and 2E). We did not observe changes in the levels of huntingtin and only mild changes of tau in GD iPS neurons, indicating that GCase mutations primarily affect α-syn levels (Figures 2E and 2F). These data confirm that endogenous mutations in GCase affect lysosomal proteolysis and cause the preferential accumulation of α-syn.

Depletion of GCase Enhances α-Syn-Mediated Neurotoxicity through Aggregation-Dependent Mechanisms

We next determined the effect of GCase KD on α-syn-mediated neurotoxicity. Because KD of GCase alone was not toxic at 7 dpi, human α-syn was overexpressed by lentiviral transduction. Immunostaining with human-specific anti-α-syn monoclonal antibodies (mAbs) syn211 and LB509 revealed the expected punctate staining pattern in neuronal extensions consistent with a synaptic enrichment of α-syn (Figure S3A) (Maroteaux et al., 1988). To examine the contribution of α-syn misfolding to neurotoxicity, we expressed the PD-linked A53T α-syn mutant as well as an artificial fibrillization-incompetent mutant, Δ71-82 α-syn (Giasson et al., 2001), in primary neurons and observed increased levels of all three variants without neurotoxicity at 7 dpi (Figure 3 and Figure S3B). By contrast, expression of human WT α-syn with GCase KD resulted in an ∼25% decline in viability by NF intensity and neuronal volume measurements compared to controls (Figures 3A and 3B). Western blot analysis with mAb syn211 of Triton X-100 soluble (T-sol) lysates indicated that α-syn protein levels increased by 1.8-fold concomitantly with the enhanced toxicity (Figure 3C). Importantly, KD of GCase also enhanced the toxicity of titer-matched A53T α-syn-infected cells to the same extent as WT α-syn, whereas no toxicity was observed in Δ71–82 α-syn-expressing neurons (Figures 3A and 3B). Toxicity by WT α-syn expression/GCase KD was further verified by measurement of condensed nuclei (Figure S3H, right). We also determined neuronal viability at later time points after infection (10 dpi) and found that toxicity was further enhanced in WT α-syn/GCase-depleted cells (∼50% viability assessed by NF intensity) (Figure S3C). Because GCase KD resulted in increased levels of A53T and Δ71–82 α-syn proteins to a similar extent as WT α-syn (Figure 3C), the toxicity appears to depend on amino acids 71–82 of α-syn, a mostly hydrophobic region that is required for α-syn polymerization (Giasson et al., 2001). Taken together, these results suggest that GCase KD promotes the accumulation and neurotoxicity of α-syn through polymerization-dependent mechanisms.

Enhanced α-Syn-Mediated Neurotoxicity by GCase Depletion Is Dependent on the Formation of Soluble and Insoluble High-Molecular-Weight Species of α-Syn

To directly determine whether GCase KD affects α-syn polymerization in neurons, lysates were sequentially extracted and separated into T-sol and -insoluble fractions followed by western blot with mAb LB509. This revealed an increase of T-sol monomeric α-syn (18 kDa), as well as T-insoluble α-syn species migrating

between 14 and 39 kDa in size upon GCase KD (Figures 3D and 3E). We next utilized native size exclusion chromatography (SEC) followed by SDS-PAGE/western blot of the collected fractions, to assess the presence of T-sol oligomeric α-syn species. GCase KD resulted in the formation of high-molecular-weight (HMW) assemblies with a molecular radius of 64–95 Å, in addition to the normal monomeric form eluting as a 31–34 Å sized particle (Figure 3F). Interestingly, analysis of Δ71–82 α-syn-expressing neurons revealed no change in the elution profile upon GCase KD (Figure 3G), further indicating that GCase KD induces the formation of a soluble HMW oligomeric α-syn that depends on the residues 71–82. These results further suggest that the ability of α-syn to form soluble oligomers and insoluble species is a critical determinant for neurotoxicity induced by GCase KD.

The increased α-syn levels and toxicity that occur with GCase depletion may result from generalized lysosomal inhibition or may be due to alterations in GlcCer lipid metabolism. To distinguish between these two possibilities, we inhibited lysosomal protein degradation with leupeptin in WT α-syn-expressing neurons and assessed neurotoxicity. We found that leupeptin treatment did not enhance α-syn-mediated neurotoxicity (Figures S3D and S3H). Biochemical analysis revealed an increase of T-insoluble α-syn in leupeptin-treated cells but no change in the amount of soluble α-syn (Figures 3D and 3E). This was corroborated by immunostaining analysis, which showed an increase in the total α-syn immunostaining intensity in leupeptin-treated compared to control cells (Figure S3F). SEC analysis also showed that soluble HMW α-syn were not detectable in neurons upon leupeptin treatment (Figure 3H), consistent with their rapid consumption into insoluble species. In addition, when comparing the increase of total α-syn (soluble and insoluble) by leupeptin treatment or GCase KD, we found that both approaches had similar effects (Figure S3F). Western blot analysis also indicated a comparable increase in the levels of LC3-II, a well-established lysosomal substrate, by leupeptin or GCase KD (Figure S3E). Thus, despite similar effects on the total α-syn levels by leupeptin or GCase KD, only GCase KD increased the steady-state levels of soluble HMW α-syn. Also, we used sequential extraction followed by SDS-PAGE/Coomassie brilliant blue (CBB) staining to determine the effect of leupeptin treatment on the solubility of total cellular proteins. Interestingly, we found that whereas leupeptin treatment increased the levels of total insoluble proteins by ∼2-fold, GCase KD had no effect (Figure S3G). This indicates that GCase KD preferentially affects the solubility of α-syn. Taken together, these data suggest that alterations in the GlcCer metabolic pathway influence the formation of toxic soluble and insoluble α-syn species, causing a stabilization of soluble HMW forms of the protein.

GlcCer Influences the Aggregation of α-Syn In Vitro by Stabilizing Soluble Oligomeric Intermediates

Because GCase KD significantly affected α-syn aggregation in neurons, we next examined whether GlcCer directly influences the in vitro aggregation of recombinant α-syn. Lipid dispersions

---

(F) Quantification of α-syn, tau, and Htt protein by western blot. Protein levels were normalized to α-tub (n = 3, values are the mean ± SEM, ***p < 0.01 compared to WT α-syn, WT and GD tau, and WT and GD Htt; *p < 0.05 compared to WT tau).
For all quantifications, values are the mean ± SEM. See also Figure S2 and Table S1.
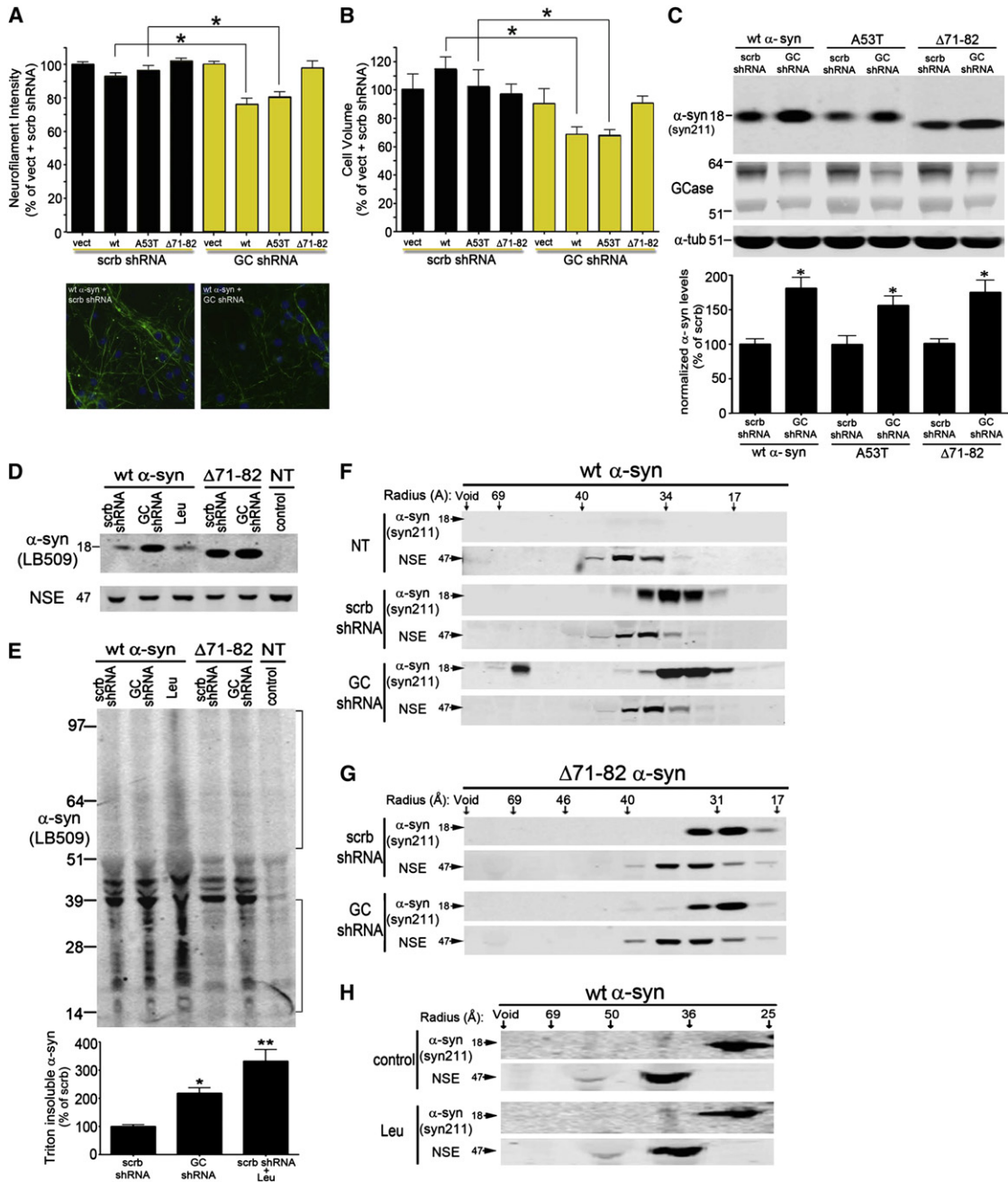
Figure 3. GCase Depletion Enhances α-Syn-Mediated Neurotoxicity through Aggregation-Dependent Mechanisms

Neurons expressing human α-syn proteins and GCase shRNA were analyzed at 7 dpi.

(A) Neurofilament immunostaining was used to monitor neurite degeneration. Representative neurofilament immunofluorescence staining (green) in WT α-syn-expressing neurons is shown below. Nuclei (DAPI) are shown in blue. Scale bars = 10 μm.

(B) Neurotoxicity was assessed by neuronal volume analysis. (for A and B: n = 8, *p < 0.001.)

(C) Protein levels of human WT, A53T, and Δ71–82 α-syn (T-sol) by western blot. α-tub was used as a loading control. Quantification is shown below (n = 6, *p < 0.01).

(D) α-Syn western blot of T-sol fractions (leu, leupeptin; NT, not transduced). NSE was used as a loading control.

(E) Western blot of T-insoluble α-syn. Quantification is shown below. The brackets show the signal used for quantification (n = 3, *p < 0.05, **p < 0.01 compared to scrb control).

(F–H) Native SEC/western blot analysis of T-sol lysates (Å, radius in angstroms). NSE was used as a loading control. Oligomeric α-syn (Void → 64 Å) was quantified (fold change: scrb shRNA = 1 ± 0.5; GC shRNA = 19.5 ± 6.0) (n = 3, values are the mean ± SEM, *p < 0.05).

MW is indicated in kDa for each blot. For all quantifications, values are the mean ± SEM. See also Figure S3.
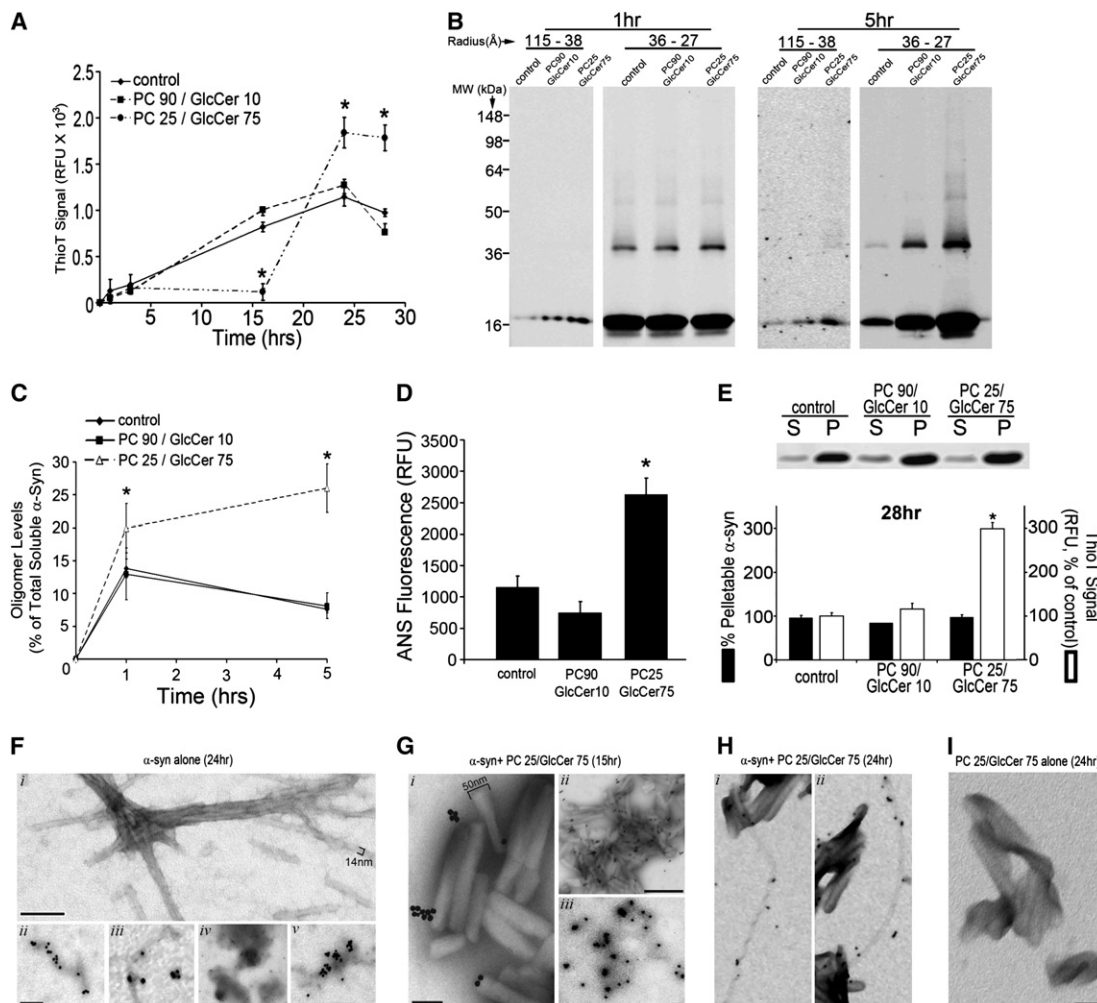
Figure 4. GlcCer Directly Influences the In Vitro Fibril Formation of Recombinant α-Syn and Stabilizes Soluble Oligomeric Species

(A) Purified α-syn was incubated with mixtures of PC and GlcCer at pH 5.0, 37°C and amyloid formation was assessed by thioflavin T fluorescence (relative fluorescence units [RFU], n = 4, *p < 0.01).

(B) Analysis of 100,000 × g soluble α-syn at 1 and 5 hr by SEC (115–38 Å and 36–27 Å fractions), then SDS-PAGE/western blot (syn211). The MW is indicated in kDa.

(C) Soluble oligomers were quantified by densitometry (n = 3, *p < 0.05).

(D) ANS fluorescence of α-syn species formed after 1 hr (n = 4, *p < 0.01).

(E) Centrifugal sedimentation analysis at 28 hr (s, supernatant; p, pellet). α-Syn was detected with Coomassie brilliant blue staining. Pelletable α-syn was quantified in the graph below (n = 3). Amyloid was measured from the same reactions by thioflavin T (n = 4, *p < 0.01).

(F) EM analysis of α-syn aggregates showing a mixture of fibrillar (i–iii) and amorphous (iv–v) structures at 24 hr. Panels ii–v show immmuno-EM analysis using mAb syn505. Scale bars: 100 nm for i–iii; 500 nm for iv and v.

(G) Immuno-EM analysis with syn505 of α-syn+PC25/GlcCer75 reactions at 15 hr. GlcCer lipid tubules are ~50 nm in width. Scale bars: 100 nm for i and iii; 500 nm for ii.

(H) Immuno-EM analysis with syn505 of α-syn+PC25/GlcCer75 reactions at 24 hr showing fibrillar structures of 10–14 nm in width with twisted (i) or straight (ii) morphologies that appear to extend from GlcCer tubules. Scale bars: 100 nm.

(I) Immuno-EM analysis of GlcCer lipid dispersions alone. Scale bar: 100 nm.

For each graph in (A) and (C)–(E), values are the mean ± SEM. See also Figure S4.

made of mixtures of purified GlcCer and brain phosphatidylcholines (PCs) were incubated with α-syn at physiological conditions (pH 7.4, 37°C). Electron microscopy (EM) analysis indicated the formation of tubules consisting of polymerized GlcCer (Figures 4G–4I), similar to those previously observed in Gaucher cells in patients and mouse models (Lee, 1968). The analysis of α-syn

aggregation under physiological conditions showed that GlcCer had no effect on fibril formation (Figure S4), consistent with previous observations (Martinez et al., 2007).

We next assessed the effect of GlcCer on α-syn fibril formation under acidic conditions (pH 5.0, 37°C) to simulate a lysosome-like environment in vitro because our neuronal culture data

indicated increased colocalization of α-syn with LAMP1 upon GCase KD (Figures S3H and S3I, Extended Discussion). These experiments revealed that acidic reactions containing lipid dispersions made of 90% PC and 10% GlcCer (PC90/GlcCer10) did not significantly influence the fibril formation of α-syn compared to control reactions containing α-syn alone (Figure 4A, Figure S4A). However, increasing the amount of GlcCer to 75% while keeping the total lipid amount constant (PC25/GlcCer75) altered the kinetic profile of α-syn fibril formation by delaying the formation of insoluble thioT-positive α-syn fibrils, extending the lag time from 2 to 16 hr (Figure 4A).

Because our biochemical data from cell culture experiments suggested that GlcCer selectively increased soluble HMW forms of α-syn (Figure 3), we hypothesized that the delay in fibril formation observed in vitro resulted from a kinetic stabilization of a soluble oligomeric intermediate species. To test this, the nature of the species that form during the lag phase (between 1 and 16 hr) of PC25/GlcCer75-containing reactions was characterized by analytic biochemical methods. Soluble portions of the reaction mixtures were obtained by centrifugation at 100,000 × g and analyzed at 1 and 5 hr after the addition of lipids by SEC/SDS-PAGE. This revealed an increase in the amount of HMW oligomeric α-syn eluting between 115 and 38 Å, and migrating at 18 kDa by SDS-PAGE, in samples containing PC25/GlcCer75 lipid dispersions (Figure 4B). Further, we detected increased amounts of soluble SDS and heat-stable dimers (36 kDa), trimers (54 kDa), and higher oligomeric species eluting as 36–27 Å-sized particles in PC25/GlcCer75-containing reactions compared to controls (Figure 4B). The GlcCer-induced soluble oligomeric species appeared to increase between 1 and 5 hr, whereas oligomers and monomers in control reactions decreased, consistent with their consumption into insoluble fibrils (Figures 4B and 4C). Native gel electrophoresis also revealed an increase in the amount of 720–1048 kDa-sized α-syn species (Figures S4C and S4D). Further, we found that other sphingolipids did not significantly alter the amounts of soluble oligomers, indicating a specific effect by GlcCer (Figures S4E and S4F). Immuno-EM with syn505 antibodies that preferentially detect misfolded α-syn demonstrated the formation of individual spherical structures of ~25–50 nm in diameter that occasionally appeared to coalesce to form larger amorphous structures (Figure 4G, iii). Syn505 also detected α-syn directly on GlcCer tubular structures (Figure 4G, i and ii) but not on GlcCer-alone reactions (Figure 4I), indicating an association of misfolded α-syn with GlcCer. α-Syn-GlcCer reactions were further analyzed by 8-anilino-1-naptha-lene sulfonate (ANS) binding, a fluorescent dye used to detect aggregation-prone conformational intermediates (Stryer, 1965). Enhanced ANS fluorescence was observed in soluble α-syn samples incubated with PC25/GlcCer75 compared to control reactions, indicating that GlcCer addition results in a conformational alteration that increases solvent-exposed hydrophobic regions (Figure 4D). Because hydrophobicity changes in proteins correlate with aggregation propensity, this observation indicates that GlcCer stabilizes the formation of a soluble assembly-competent intermediate species during the lag phase of the fibril formation reaction.

Further inspection of the kinetic profile indicated that although GlcCer delayed the onset of fibril formation from 2 to 16 hr, it also accelerated fibril assembly once this phase was initiated (Figure 4A). The fibril assembly phase of PC25/GlcCer75-containing reactions occurred between 16 and 24 hr, compared to control reactions where the assembly occurred between 2 and 24 hr. Furthermore, the maximal thioT signal at the end stages of the reaction was 2- to 3-fold higher compared to control reactions (Figure 4A). We further analyzed the aggregated species formed at the end stage of the fibril-forming reaction, after assembly was completed and equilibrium was reached (at 28 hr). Centrifugal sedimentation analysis at 100,000 × g, which detects both amyloid and non-amyloid aggregates in the pelletable (P) fractions, revealed that GlcCer had no effect on the amount of pelletable α-syn protein (Figure 4E). In the same reaction mixtures used for sedimentation analysis, measurement of amyloidogenic α-syn with thioT revealed a 3-fold increase in the amount of amyloid detected in PC25/GlcCer75-containing reactions (Figure 4E, bottom). Immuno-EM analysis of α-syn/GlcCer reactions at 24 hr confirmed the presence of ~14 nm wide fibrillar structures that appeared to extend from GlcCer tubules (Figure 4H), whereas α-syn-alone reactions contained both fibrillar (Figure 4F, i–iii) as well as amorphous aggregates (Figure 4F, iv and v). Taken together, these data indicate that GlcCer selectively stabilizes the formation of soluble oligomeric intermediates on-pathway to forming amyloid fibrils. However, due to the continuous accumulation of these soluble on-pathway intermediates that occurs in vitro between 2 and 16 hr, the concentration of GlcCer is likely eventually surpassed and results in the rapid formation of thioT-positive amyloid fibrils.

Accumulation of Soluble and Insoluble α-Syn Species Occurs in GD Mouse

As GlcCer appears to affect the levels of soluble α-syn oligomers in neuronal cultures and in vitro, we next examined whether GCase depletion and GlcCer accumulation affect α-syn levels and soluble oligomer formation in vivo. For this, brain tissues from a previously described GD mouse model (4L/PS-NA) were analyzed to determine whether endogenously expressed α-syn protein levels were elevated. Previous analysis of this mouse model indicated low levels of GCase activity, neuronal accumulation of GlcCer, and severe neurological deterioration by 20 weeks of age (Sun et al., 2005). In addition to GlcCer, the levels of other sphingolipids were also determined showing an accumulation of lactosylceramide, GM2, and GD3, whereas ceramide levels remained unchanged (Figures S5A and S5B). Our neuropathological analysis revealed the presence of eosinophilic spheroids, suggesting the presence of degenerating neurons, in multiple brain regions including the substantia nigra (SN) and cortex (Ctx) in GD mice compared to WT mice that exhibited normal neuronal architecture (Figures 5A and 5D). These degenerative changes occurred concomitantly with increased levels of α-syn in these regions (Figure 5B). Immunofluorescence analysis revealed the presence of α-syn accumulations in the form of punctated structures (<5 μm in diameter), whereas WT mice showed a normal neuropil staining pattern expected for α-syn (Figures 5B–5D). These changes were not restricted to the SN and Ctx, as α-syn accumulations were also observed in other neural regions including cerebellum, hippocampus, and brainstem (Xu et al., 2010).

Additionally, both intraneuronal and extraneuronal α-syn accumulations were identified by costaining with the neuron-specific marker NeuN (Figure 5C), whereas quantitative analysis did not reveal significant neuronal loss (Figure 5D). The solubility of α-syn was analyzed in 4L/PS-NA by sequential extraction in Triton X-100 buffer, then 2% SDS buffer. Both syn202 and SNL-1, antibodies that detect total α-syn, revealed increased levels of T-sol α-syn in 4L/PS-NA mice compared to WT mice (Figures 5E, left, and 5F). T-insoluble fractions showed the expected low levels of α-syn in WT mice and more aggregated α-syn in 4L/PS-NA mice as detected with both syn202 and syn505 (Figures 5E, right, and 5F). Analysis of T-sol levels by SEC showed increased levels of putative oligomeric forms (120–70 Å- and 51–44 Å-sized species), whereas monomers were similar to control mice (Figures 5G and 5H). Quantification of the soluble HMW α-syn revealed a 4-fold increase in 4L/PS-NA mice compared to control mice (Figures 5F and 5H). We confirmed our analysis of α-syn in another previously described and well-characterized GD mouse model, GCase harboring the GD-linked D409H loss-of-function mutation (Xu et al., 2003). This revealed that D409H mice had similar increases in α-syn punctated structures as observed by immunostaining analysis (Figure S5C) as well as higher levels of soluble oligomers and insoluble α-syn species (Figure S5D). Finally, we used a well-established *C. elegans* model to further demonstrate that depletion of GCase causes the accumulation of α-syn in vivo (Figure S5E). Taken together, these data are consistent with our cell culture and in vitro data demonstrating that GCase depletion promotes the formation of soluble oligomeric and insoluble α-syn in vivo.

Elevated Levels of Soluble HMW α-Syn in GD Brain Are Associated with Neurodegeneration

Because our in vitro, cell culture, and GD animal model data suggested that GlcCer accumulation leads to elevated levels of soluble α-syn oligomers, we next sought to identify these species in human postmortem brain samples obtained from patients with GD. T-sol fractions of cortical samples were analyzed by native SEC, followed by SDS-PAGE/western blot of the collected fractions using mAb syn211. Analysis of healthy controls without *GBA1* mutations (Table S2) revealed the expected elution profile typically observed for monomeric human α-syn, eluting mainly as a 34 Å-sized particle by SEC and migrating at 18 kDa by SDS-PAGE (Figures 6A–6C). Analysis of cortical T-sol lysate from two pathologically and clinically confirmed non-neuronopathic type I GD patients revealed an α-syn elution profile that was similar to control (Figures 6D and 6E), although the total levels of monomeric α-syn were elevated (α-syn protein levels, % of control): control = 100 ± 12.6, GD type I (no PD) = *243 ± 53,values are the mean ± standard error of the mean (SEM),*p < 0.05, n = 3 controls, n = 2 GD type I). When brain lysate from a previously documented GD patient diagnosed with atypical Parkinson's disease (APD) was analyzed (Tayebi et al., 2001), a dramatic increase in α-syn levels was observed (Figure 6F). α-Syn eluted as a 34 Å-sized particle and migrated at 18 kDa by SDS-PAGE similar to controls, but a substantial proportion (50% of the total T-sol) also eluted as a larger putative oligomeric species

at 42–45 Å (or 110–140 kDa globular protein). The α-syn in this oligomeric fraction, when analyzed by denaturing SDS-PAGE, resolved as 22, 44, and 75 kDa heat-stable species (Figure 6F). These data demonstrate that elevated T-sol α-syn in the form of oligomeric species is present primarily in the GD/APD brain.

We also detected elevated levels of α-syn oligomers in patients that were homozygous or heterozygous for GCase mutations (Table S2) with a diagnosis of Lewy body dementia (DLB) (Figures 6G and 6K). Analysis of postmortem brain lysate obtained from infants diagnosed with type II GD as well as a 3-year-old child diagnosed with type III GD also exhibited increased oligomeric α-syn eluting above 36 Å (Figures 6H–6J), although some variation between samples was observed. We quantified the levels of oligomeric α-syn detected with the syn211 mAb and found that both homozygote and heterozygote carriers of *GBA1* mutations with a neuronopathic phenotype contained significantly higher levels of oligomers compared to controls (Figure S6C). We also verified that these GD samples contained lower GCase protein and activity levels (Figures S6A, S6B, and S6E). Taken together, the data suggest that GCase deficiency promotes the formation of oligomeric α-syn, and the occurrence of these oligomers in type II and type III GD brain suggests that they may also play a role in the pathogenesis of age-independent, infantile GD forms.

We further analyzed the 45 Å-sized oligomeric fractions with mAb syn303, an antibody that preferentially detects pathological oligomeric α-syn (Duda et al., 2002) and can distinguish potentially toxic from nontoxic α-syn species (Tsika et al., 2010). We found that syn303 immunoreactivity was increased in all of the neuronopathic GD samples (Figure 6L, Figure S6D). In most of the cases, syn303 reacted with the 22, 44, and 75 kDa species that were also detected with syn211 (Figure 6L). These data further demonstrate that toxic oligomeric α-syn is elevated in patients harboring *GBA1* mutations and is preferentially associated with neuronopathic forms of the disease.

Overexpression of α-Syn Inhibits the Intracellular Trafficking of GCase Resulting in Decreased Lysosomal GCase Activity

Although most patients with idiopathic PD invariably have elevated levels of α-syn protein, they do not harbor mutations in the *GBA1* gene and thus are expected to have normal lysosomal function of GCase. However, recent evidence in *S. cerevisae* and cell lines indicated that overexpression of α-syn has the ability to impede ER–Golgi trafficking of proteins, by inhibiting the formation of soluble N-ethylmaleimide-sensitive factor attachment protein receptor (SNARE) protein complexes (Cooper et al., 2006; Thayanidhi et al., 2010). To determine whether α-syn disrupts lysosomal maturation and activity of GCase, we overexpressed α-syn in H4 cells and primary cortical neurons that express WT GCase and measured the post-ER forms. The intracellular trafficking of GCase was assessed by SDS-PAGE/western blot, through molecular weight (MW) analysis of various GCase forms that result from protein glycosylation. Whereas the ER form of GCase migrates at 60 kDa, the post-ER GCase forms migrate above 60 kDa (Erickson et al., 1985). Analysis of whole-cell lysates from
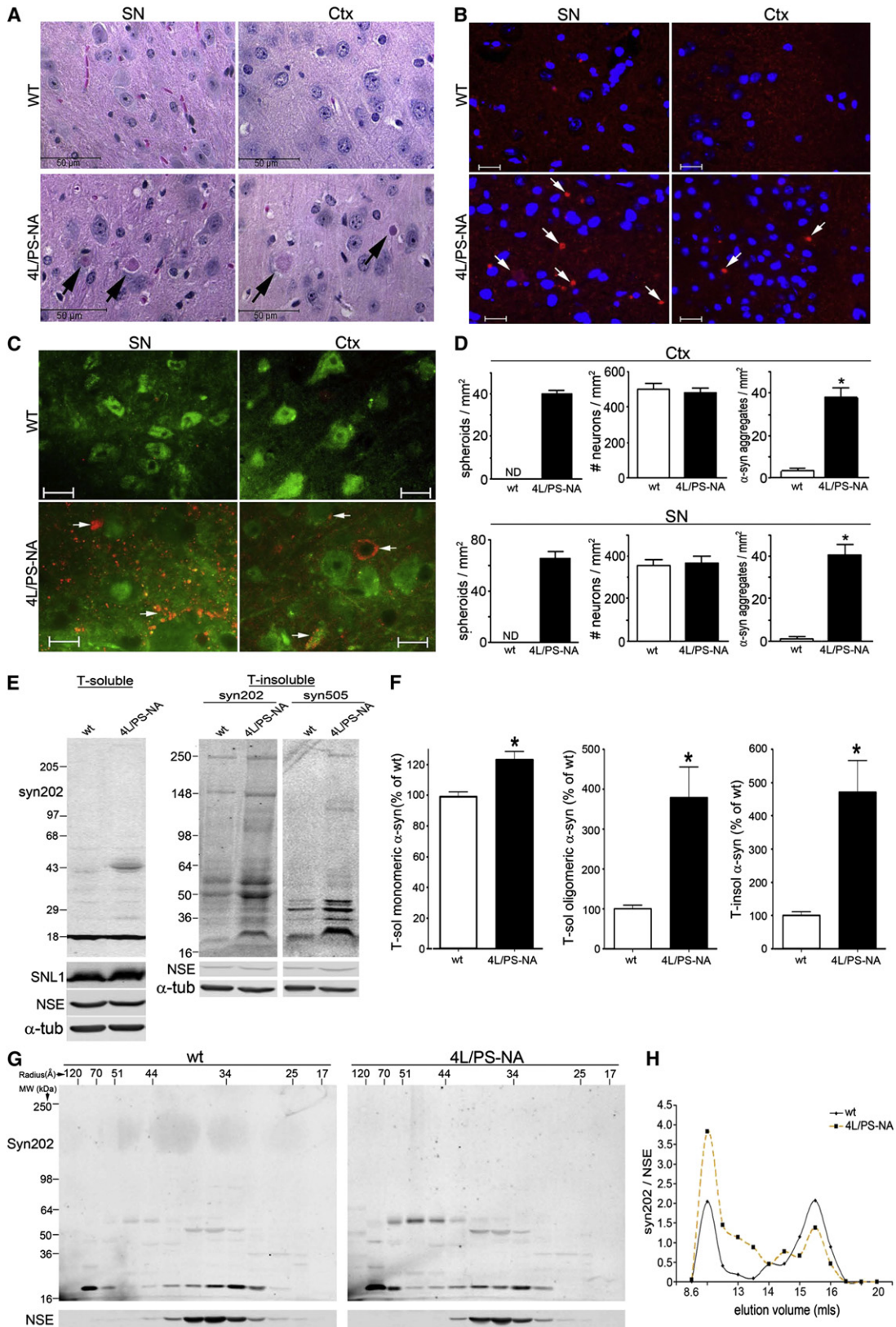
inducible H4 cells showed that lowering α-syn expression levels by the addition of dox for 24 or 32 hr resulted in a concomitant increase in the post-ER GCase forms while decreasing the 60 kDa ER form (Figure 7A). Similarly, overexpression of human WT and A53T α-syn in primary cortical neurons also altered the post-ER/ER GCase ratio by causing an accumulation of the ER form, as well as a decrease in the post-ER forms migrating above 60 kDa (Figure 7B). Titer-matched infection of WT and A53T α-syn containing plasmids resulted in almost equal alterations in the post-ER/ER GCase ratio, despite the lower protein expression of A53T, indicating that A53T more potently inhibits GCase trafficking compared to the WT protein (Figure 7B). Interestingly, expression of Δ71–82 α-syn at levels that were slightly higher than WT α-syn caused only a mild alteration in the post-ER/ER GCase ratio that was not significantly different compared to empty vector controls (Figure 7B). To verify that alterations in GCase glycoslyation patterns observed by western blot corresponded to lower lysosomal activity of GCase, enzymatic activity was measured in lysosomal (P2) and microsomal (P3) enriched fractions (Figures S7A and S7B) of primary neuronal cultures. In P2 fractions, expression of both WT and A53T α-syn resulted in a significant decrease in GCase activity and a concomitant increase in the P3 activity compared to controls (Figure 7C). Conversely, the expression of Δ71–82 α-syn did not affect GCase lysosomal activity (Figure 7C). The results were validated by endo H treatment of lysates, which revealed higher levels of endo H-sensitive GCase migrating below 60 kDa in endo H-treated samples of WT α-syn-expressing cells compared to control conditions (Figure S7C). Additionally, we tested the ability of another amyloid-forming protein, poly Q-expanded huntingtin fragment 548–72Q, to inhibit GCase maturation and found no change (Figure S7C). Finally, we confirmed that the accumulation of ER GCase by α-syn occurred at the protein level, as measurement of GBA1 mRNA of α-syn-expressing neurons was not different compared to control conditions (Figure S7D). The enzymatic activity of other lysosomal proteins in the P2 fraction of infected neurons revealed only minor alterations by α-syn expression, suggesting a preferential effect of α-syn on GCase activity (Figure S7E).

To determine whether GCase glycosylation patterns are sensitive to α-syn protein levels in vivo, human cortical material was analyzed by GCase western blot. Upon analyzing brain tissue from several reportedly healthy controls without common

GBA1 mutations and between the ages of 65 and 80 years of age (Table S3 and Table S4), we noticed a natural variability of α-syn expression levels between subjects. Control samples 1, 2, 4, and 6 were noted to have mid-to-high levels of α-syn relative to samples 3 and 5, which contained very low α-syn levels (Figure 7D). When the GCase glycosylation patterns were analyzed by western blot, we observed a dramatic difference in the post-ER/ER GCase ratio that correlated with α-syn levels. While all samples appeared to have similar levels of post-ER GCase, samples with low α-syn (samples 3 and 5) contained much less of the 60 kDa ER form (Figure 7D). Endo H digestion also confirmed higher levels of ER-containing GCase, which migrated below 60 kDa after endo H treatment (Figure S7F). We further analyzed the GCase activity levels in cortical tissue from whole-cell lysates of all low and high α-syn-containing samples and found no difference in activity (Figure S7H, left). However, when P2 and P3 GCase activity was determined, we found that microsome-enriched P3 fractions of "high" α-syn samples contained significantly higher levels of activity whereas no change was observed in the P2 fraction (Figure S7H). Western blot analysis with syn303 also revealed higher levels of oligomeric, oxidized α-syn in "high" α-syn sample C6 compared to C5 (Figure S7G). These findings suggest that normal variation of α-syn protein levels modulate the lysosomal maturation and activity GCase in vivo.

The observation that elevated α-syn levels affect GCase trafficking in neurons led us to hypothesize that lysosomal GCase function may be lowered in idiopathic PD brain. We found an ~40% decline in the total GCase protein levels in T-sol lysates from cingulate cortex of PD brain when compared to age- and postmortem time-matched controls (Figure 7E). In addition, there was an ~50% decline in GCase activity in the P2 fraction relative to age-matched controls, whereas no change was observed in the P3 fraction (Figure 7E, bottom). Genotyping analysis revealed that these patients did not harbor mutations in GBA1, with the exception of one sample that contained the heterozygous mutation N370S (Table S5). This one sample, PD4, had lower than the expected 50% decline in GCase activity (38% of control), possibly indicating additional inhibition of GCase by α-syn accumulation (Table S6). Taken together, these data suggest that elevated levels of α-syn observed in PD and other synucleinopathies lead to decreased lysosomal activity of normal GCase that may in turn contribute to further propagation and stabilization of oligomeric α-syn.

Figure 5. α-Syn Accumulation and Soluble Oligomer Formation in GD Mice
Analysis of 12-week-old GD mice (4L/PS-NA).
(A) H & E stain of the substantia nigra (SN) and cortex (Ctx). The arrows indicate eosinophilic spheroids. Scale bars = 50 μm.
(B) Immunofluorescence of α-syn (red) in SN and Ctx. Nuclei are stained with DAPI (blue). Scale bars = 20 μm.
(C) Costaining of α-syn (red) and neuronal marker NeuN (green). Scale bars = 20 μm.
(D) Left: Quantification of neuronal spheroids. ND, not detected. Middle: Quantification of neuronal number by NeuN immunostaining. Right: Quantification of α-syn aggregates by immunostaining.
(E) Sequential extraction analysis of Ctx. pAb SNL-1 and mAb syn202 detect total endogenous α-syn, whereas syn505 detects oxidized/nitrated and misfolded α-syn. NSE and α-tub were used as loading controls.
(F) Quantification of T-sol monomers (18 kDa, left), T-sol oligomers (>18 kDa, middle), and T-insoluble α-syn (total lane, right).
(G) Native SEC/SDS-PAGE/western blot of T-sol fractions. Radius, Å.
(H) Chromatographic profile obtained by syn202 densitometry. The values are representative of independent SEC analyses from three mice. The MW is indicated in kDa for each blot. For all quantifications, values are the mean ± SEM.
See also Figure S5.
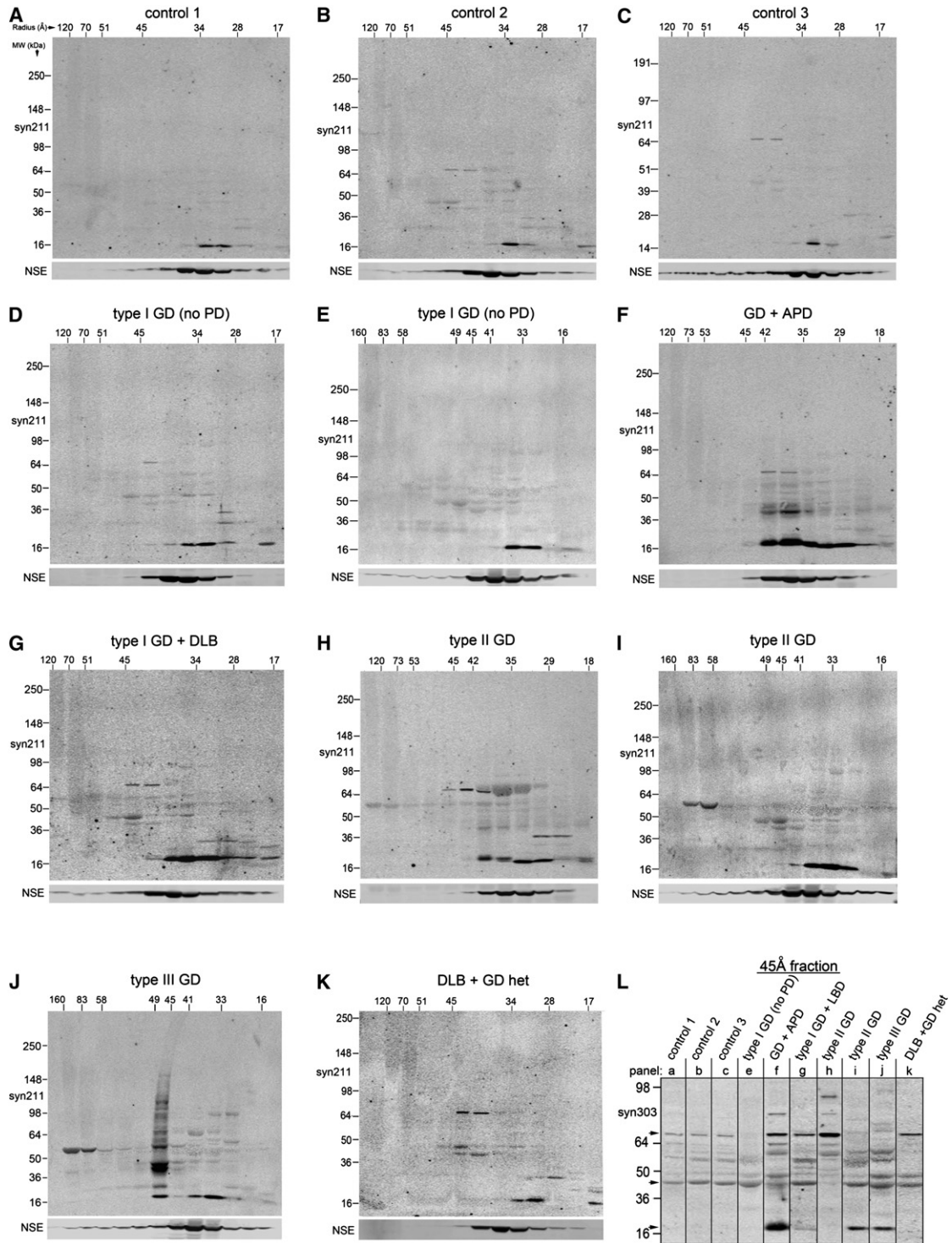
Figure 6. Accumulation of T-Sol α-Syn Oligomers Occurs in GD Brain

Native SEC followed by SDS-PAGE/western blot of human cortical lysates (T-sol). Radius is in Å (horizontal), apparent MW is in kDa (vertical). Monomeric α-syn elutes at 34 Å.

(A–C) Healthy controls.

(D and E) Type I non-neuronopathic GD.

(F) Atypical Parkinson's disease (APD).

(G) dementia with Lewy bodies (DLB).

DISCUSSION

Our data indicate that deficient GCase leads to accumulation of GlcCer in neurons that in turn promotes formation of toxic α-syn oligomers. GCase depletion causes a decline in lysosomal proteolysis that preferentially affects α-syn (Figures 1E and 1F). It is likely that the unique inherent property of α-syn to form amyloid fibrils plays a critical role in the neurotoxicity that occurs with GCase KD, as expression of α-syn mutant lacking the 71–82 region did not affect neuronal viability in our culture model (Figure 3). Interestingly, another aggregation-prone protein involved in neurodegenerative disorders, tau, did not accumulate (Figure 1 and Figure 2), indicating that GCase function is preferentially related to α-syn. Importantly, similar results were observed in human iPS neurons in the presence of endogenous mutations in GCase, suggesting that GCase protein depletion or expression of loss-of-function GCase mutants exhibit comparable phenotypes.

Biochemical analysis indicated that GCase KD caused a dramatic increase in the levels of soluble oligomers (Figure 3). This effect was distinct from that observed by leupeptin, which primarily resulted in elevated levels of T-insoluble α-syn without altering soluble forms. This suggests that in addition to general lysosomal inhibition, GlcCer accumulation specifically affects the conformation and solubility of α-syn by stabilizing the levels of soluble intermediates. In vitro studies using purified recombinant α-syn demonstrated that GlcCer has the ability to prolong the lag phase of fibril growth and stabilize oligomeric intermediates only at acidic pH (Figure 4 and Figure S4). This pH-dependent effect is consistent with accumulation of α-syn within LAMP1-positive vesicles and subcellular fractions upon GCase KD (Figures S3H and S3I). After the lag phase, GlcCer accelerated amyloid formation and formed fibrils that appeared to extend from GlcCer lipid tubules (Figure 4H). It is possible that GlcCer tubules provide a scaffold or platform for oligomeric intermediates to form that, once saturated, proceed to rapid polymerization of fibrils. This ability may be a crucial step in pathogenesis, as the documentation of α-syn oligomers appears to be correlated with neurodegeneration in neuronal cultures, mouse models, and human neuronopathic GD brain.

SEC analysis of postmortem GD and PD brain demonstrated elevated levels of a previously undocumented 36–45 Å-sized soluble oligomeric α-syn species that correlated with a neurological phenotype. The oligomers prominently reacted with the mAb syn303, an antibody generated against oxidized/nitrated α-syn that preferentially detects pathological conformations of the protein that exhibit toxic properties (Tsika et al., 2010). The pathological α-syn oligomers were also detected in infantile neuronopathic GD cases, and in a child with type III GD (Figure 6), strongly suggesting that GBA1 mutations and specific alter-

ations in the GlcCer metabolism pathway influence α-syn oligomerization that is not necessarily age dependent.

The absence of oligomeric α-syn in samples from type I GD without parkinsonism (Figures 6D and 6E) indicates that other factors, in addition to deficiency of GCase, likely contribute to oligomerization of α-syn in neuronopathic GD. For example, oxidation and nitration of α-syn have been shown to impede clearance and stabilize α-syn oligomers in vitro (Hodara et al., 2004), and chaperones have also been shown to abrogate α-syn toxicity and aggregation (Auluck et al., 2002). Although our analysis of GD brain indicated increased levels of oxidized α-syn in neuronopathic forms (Figure 6L), further studies are required to examine how oxidation and other age-dependent processes interact with deficiency of GCase in promoting α-syn oligomerization.

Our data also demonstrate that elevated α-syn inhibits intracellular trafficking and lysosomal function of normal GCase in neurons (Figure 7 and Figure S7). This indicates that decreased GCase activity not only contributes to toxicity in patients with GBA1 mutations but also may affect the development of more common sporadic forms of PD and synucleinopathies that do not have mutations in the GBA1 gene. Interestingly, we show that variation of α-syn levels in healthy control subjects can also alter ER-Golgi flux of GCase, a property that may be potentiated by α-syn oligomerization. This is further suggested by normal GC activity in neurons expressing aggregation-incompetent Δ71–82-α-syn (Figure 7C) as well as the increased immunoreactivity to syn303 in controls that contain higher levels of ER GCase (Figure S7G). However, further studies are required to delineate the precise mechanism of α-syn-mediated inhibition of GCase maturation.

Taken together, our results suggest that elevated levels of toxic α-syn species lead to depletion of lysosomal GCase and further stabilization of α-syn oligomers by GlcCer accumulation. This self-propagating positive feedback process proceeds until a pathogenic threshold is surpassed, resulting in neurodegeneration (Figure 7F). Therefore, specific treatments that promote targeting of GCase to lysosomes are expected to diminish the formation of toxic α-syn oligomers and break the pathogenic cycle of α-syn aggregation and toxicity in PD and other synucleinopathies.

EXPERIMENTAL PROCEDURES

Primary Cortical Cultures, Lentiviral Infection, and Leupeptin Treatment

Primary cortical culture procedures have been described in detail previously (Tsika et al., 2010). Cells were infected at a multiplicity of infection (moi) of 3 for both GCase shRNA and α-syn-expressing lentivirus. For leupeptin treatment, cells were infected with α-syn-expressing lentivirus at days in vitro (DIV) 5, then treated with 50 μM leupeptin (EMD chemicals, http://www.emdchemicals.com) at DIV 8, and harvested at DIV 12 (or dpi 7).

(H and I) Analysis of cortical material obtained from infants with type II acute neuronopathic GD.
(J) Cortical lysates from a 3-year-old child with neuronopathic type III GD.
(K) DLB with a heterozygous mutation in GBA1.
(L) Analysis of the 45 Å-sized fraction with syn303, which preferentially detects pathological oligomeric α-syn. Bands migrating at 18, 44, and 75 kDa were detected with both syn303 and syn211 (arrows).
See also Figure S6 and Table S2.
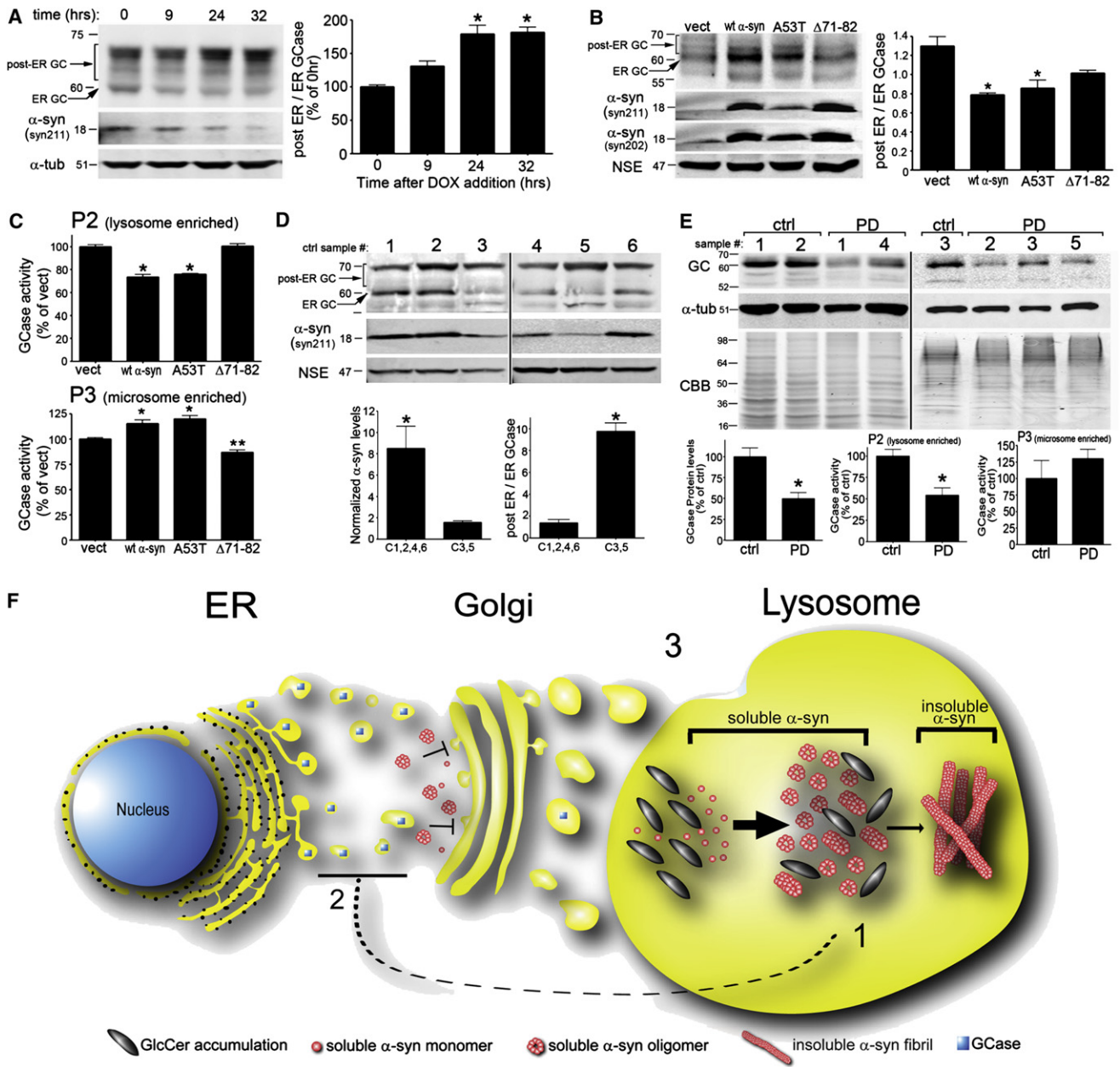
Figure 7. Elevated Levels of α-Syn Inhibit the Intracellular Trafficking of GCase and Decrease Lysosomal GCase Function

(A) Inducible H4 cells expressing human WT α-syn were analyzed by western blot for post-ER and ER GCase (n = 6, *p < 0.01). α-tub was used as a loading control.

(B) post-ER/ER GCase in cortical neurons expressing human WT, A53T, or Δ71–82 α-syn. α-syn levels were determined by syn211 (human-specific) and syn202 (human and mouse). NSE was used as a loading control.

(C) GCase activity in cortical neurons of P2 and P3 fractions (n = 6, *p < 0.01, compared to vect).

(D) Analysis of GCase in cortex of 65- to 80-year-old controls. Samples 1, 2, 4, 6 = "high α-syn"; samples 3, 5 = "low α-syn." Quantification of α-syn protein and post-ER/ER GCase levels is graphed below the blots (*p < 0.01).

(E) GCase western blot of PD brain lysates. α-Tub and CBB were used as loading controls. GCase levels were quantified below (n = 3 [control] or 6 [PD], *p = 0.02). Bottom: GCase activity in P2 and P3 fractions (n = 3–6, *p = 0.04). MW for each blot is indicated in kDa.

(F) Pathogenic positive feedback mechanism of α-syn and GCase depletion in the lysosome. (1) Lysosomal GlcCer accumulation accelerates and stabilizes soluble α-syn oligomers (bold arrow), which eventually convert into amyloid fibrils (thin arrow). (2) Accumulation of α-syn blocks the ER-Golgi trafficking of GCase. (3) Decrease of GCase in the lysosome further amplifies GlcCer accumulation and stabilization of soluble α-syn oligomers and results in a stronger inhibition of GCase ER-Golgi trafficking with each pathogenic cycle. For all quantifications, values are the mean ± SEM. See also Figure S7 and Table S3, Table S4, Table S5, and Table S6.

Proteolysis Measurements

Proteolysis of long-lived proteins was determined by radioactive pulse-chase using H^3-leucine (Extended Experimental Procedures).

Neurotoxicity Assessment

Cortical cells were seeded in 96-well plates at 50,000 cells/well, infected at DIV 5, and fixed in 4% paraformaldehyde at the indicated time points. The staining and analysis procedures have been described (Tsika et al., 2010).

Sequential Biochemical Extraction of Cell Cultures and Tissues

Cells were harvested in Triton X-100 lysis buffer. The extracts were centrifuged at 100,000 × g for 30 min. The pellets were extracted in 2% SDS buffer. Similar procedures were utilized for mouse and human brain tissues, using 20 volumes of Triton X-100 lysis buffer. Samples were loaded onto SDS-PAGE gels or subjected to native SEC followed by western blot analysis (Extended Experimental Procedures) (Mazzulli et al., 2006).

Native SEC

Infected cortical cells (8,000,000 cells/10 cm plate) were harvested in Triton X-100 lysis buffer and 100,000 × g Triton X-100 soluble lysate was loaded onto a Superdex 200 HR 10/300 column (GE healthcare, http://www.gelifesciences.com) as described previously (Mazzulli et al., 2006). Quantification of α-syn oligomers has been described in detail previously (Tsika et al., 2010).

α-Synuclein Protein Purification and Amyloid Measurements

Recombinant human α-syn was purified from BL21 CodonPlus (DE3)-RIL competent *E. coli* (Agilent) as described previously (Mazzulli et al., 2007). Purified α-syn was mixed with lipid dispersions (see Extended Experimental Procedures) and amyloid formation was determined by thioflavin T binding as described in the Supplemental Information.

Histological Analysis of Gaucher Disease Mouse Models

The homozygous point-mutated *gba1* mice expressing V394L (4L) crossed to the hypomorphic prosaposin mutant mice (PS-NA) have been described previously (Sun et al., 2005). Histological analyses are described in the Extended Experimental Procedures.

Subcellular Fractionation

Infected cortical cells (8,000,000 cells/10 cm plate) were harvested in 0.25 M sucrose buffer containing 10 mM HEPES (pH 7.4) and 0.1M EDTA (SHB), homogenized, and centrifuged at 6,800 × g, 4°C, for 5 min. The remaining pellet was saved (P1). The supernatant was centrifuged at 17,000 × g, 4°C, for 10 min, supernatant removed (S), and the remaining pellet (P2) enriched in lysosomes was saved. Fraction S was centrifuged at 100,000 × g for 1 hr to obtain P3. Pellets were extracted in 1% Triton X-100 lysis buffer, then 2% SDS buffer as described above. Fractions were analyzed by western blot analysis or by measuring GCase activity (Extended Experimental Procedures).

Statistical Analysis

One-way ANOVA with Tukey's post-hoc test was used in proteolysis, neurotoxicity, immunostaining quantifications of LC3 and α-syn, P2 and P3 GCase activity assays, ANS, and thioflavin T determinations. One-way ANOVA with Dunnet's post-hoc test was used for post-ER/ER GCase ratios of cortical neurons. Two-tailed Student's t test was utilized for biochemical analyses, quantification of α-syn and GCase protein levels, BODIPY 493 fluorescence analysis, and lipidomic analysis. p values less than 0.05 were considered significant. Statistical calculations were performed with GraphPad Prism Software, Version 4.0 (http://www.graphpad.com).

SUPPLEMENTAL INFORMATION

Supplemental Information includes Extended Discussion, Extended Experimental Procedures, seven figures, and six tables and can be found with this article online at doi:10.1016/j.cell.2011.06.001.

REFERENCES

Auluck, P.K., Chan, H.Y., Trojanowski, J.Q., Lee, V.M., and Bonini, N.M. (2002). Chaperone suppression of alpha-synuclein toxicity in a Drosophila model for Parkinson's disease. Science *295*, 865–868.

Brady, R.O., Kanfer, J., and Shapiro, D. (1965). The metabolism of glucocerebrosides. I. Purification and properties of a glucocerebroside-cleaving enzyme from spleen tissue. J. Biol. Chem. *240*, 39–43.

Bultron, G., Kacena, K., Pearson, D., Boxer, M., Yang, R., Sathe, S., Pastores, G., and Mistry, P.K. (2010). The risk of Parkinson's disease in type 1 Gaucher disease. J. Inherit. Metab. Dis. *33*, 167–173.

Chandra, S., Gallardo, G., Fernandez-Chacon, R., Schluter, O.M., and Sudhof, T.C. (2005). Alpha-synuclein cooperates with CSPalpha in preventing neurodegeneration. Cell *123*, 383–396.

Conway, K.A., Harper, J.D., and Lansbury, P.T. (1998). Accelerated in vitro fibril formation by a mutant alpha-synuclein linked to early-onset Parkinson disease. Nat. Med. *4*, 1318–1320.

Cooper, A.A., Gitler, A.D., Cashikar, A., Haynes, C.M., Hill, K.J., Bhullar, B., Liu, K., Xu, K., Strathearn, K.E., Liu, F., et al. (2006). Alpha-synuclein blocks ER-Golgi traffic and Rab1 rescues neuron loss in Parkinson's models. Science *313*, 324–328.

Duda, J.E., Giasson, B.I., Mabon, M.E., Lee, V.M., and Trojanowski, J.Q. (2002). Novel antibodies to synuclein show abundant striatal pathology in Lewy body diseases. Ann. Neurol. *52*, 205–210.

Erickson, A.H., Ginns, E.I., and Barranger, J.A. (1985). Biosynthesis of the lysosomal enzyme glucocerebrosidase. J. Biol. Chem. *260*, 14319–14324.

Giasson, B.I., Murray, I.V., Trojanowski, J.Q., and Lee, V.M. (2001). A hydrophobic stretch of 12 amino acid residues in the middle of alpha-synuclein is essential for filament assembly. J. Biol. Chem. *276*, 2380–2386.

Giasson, B.I., Duda, J.E., Quinn, S.M., Zhang, B., Trojanowski, J.Q., and Lee, V.M. (2002). Neuronal alpha-synucleinopathy with severe movement disorder in mice expressing A53T human alpha-synuclein. Neuron *34*, 521–533.

Goker-Alpan, O., Schiffmann, R., LaMarca, M.E., Nussbaum, R.L., McInerney-Leo, A., and Sidransky, E. (2004). Parkinsonism among Gaucher disease carriers. J. Med. Genet. *41*, 937–940.

Goker-Alpan, O., Giasson, B.I., Eblan, M.J., Nguyen, J., Hurtig, H.I., Lee, V.M., Trojanowski, J.Q., and Sidransky, E. (2006). Glucocerebrosidase mutations are an important risk factor for Lewy body disorders. Neurology *67*, 908–910.

Grabowski, G.A. (2008). Phenotype, diagnosis, and treatment of Gaucher's disease. Lancet *372*, 1263–1271.

Hodara, R., Norris, E.H., Giasson, B.I., Mishizen-Eberz, A.J., Lynch, D.R., Lee, V.M., and Ischiropoulos, H. (2004). Functional consequences of alpha-synuclein tyrosine nitration: diminished binding to lipid vesicles and increased fibril formation. J. Biol. Chem. *279*, 47746–47753.

Kayed, R., Head, E., Thompson, J.L., McIntire, T.M., Milton, S.C., Cotman, C.W., and Glabe, C.G. (2003). Common structure of soluble amyloid oligomers implies common mechanism of pathogenesis. Science *300*, 486–489.

Lee, R.E. (1968). The fine structure of the cerebroside occurring in Gaucher's disease. Proc. Natl. Acad. Sci. USA *61*, 484–489.

Lill, C.M., Roehr, J.T., McQueen, M.B., Bagade, S., Kavvoura, F., Schjeide, B.M.M., Allen, N.C., Tanzi, R., Khoury, M.J., Ioannidis, J.P.A., and Bertram, L. (2008). The PDGene Database. Alzheimer Research Forum. Available at: http://www.pdgene.org Accessed 09/2008–03/2009.

Manning-Bog, A.B., Schule, B., and Langston, J.W. (2009). Alpha-synuclein-glucocerebrosidase interactions in pharmacological Gaucher models: a biological link between Gaucher disease and parkinsonism. Neurotoxicology 30, 1127–1132.

Maroteaux, L., Campanelli, J.T., and Scheller, R.H. (1988). Synuclein: a neuron-specific protein localized to the nucleus and presynaptic nerve terminal. J. Neurosci. 8, 2804–2815.

Martinez, Z., Zhu, M., Han, S., and Fink, A.L. (2007). GM1 specifically interacts with alpha-synuclein and inhibits fibrillation. Biochemistry 46, 1868–1877.

Mazzulli, J.R., Mishizen, A.J., Giasson, B.I., Lynch, D.R., Thomas, S.A., Nakashima, A., Nagatsu, T., Ota, A., and Ischiropoulos, H. (2006). Cytosolic catechols inhibit alpha-synuclein aggregation and facilitate the formation of intracellular soluble oligomeric intermediates. J. Neurosci. 26, 10068–10078.

Mazzulli, J.R., Armakola, M., Dumoulin, M., Parastatidis, I., and Ischiropoulos, H. (2007). Cellular oligomerization of alpha-synuclein is determined by the interaction of oxidized catechols with a C-terminal sequence. J. Biol. Chem. 282, 31621–31630.

Neudorfer, O., Giladi, N., Elstein, D., Abrahamov, A., Turezkite, T., Aghai, E., Reches, A., Bembi, B., and Zimran, A. (1996). Occurrence of Parkinson's syndrome in type I Gaucher disease. QJM 89, 691–694.

Neumann, J., Bras, J., Deas, E., O'Sullivan, S.S., Parkkinen, L., Lachmann, R.H., Li, A., Holton, J., Guerreiro, R., Paudel, R., et al. (2009). Glucocerebrosidase mutations in clinical and pathologically proven Parkinson's disease. Brain 132, 1783–1794.

Seibler, P., Graziotto, J., Jeong, H., Simunovic, F., Klein, C., and Krainc, D. (2011). Mitochondrial parkin recruitment is impaired in neurons derived from mutant PINK1 induced pluripotent stem cells. J. Neurosci. 31, 5970–5976.

Sidransky, E. (2005). Gaucher disease and parkinsonism. Mol. Genet. Metab. 84, 302–304.

Sidransky, E., Nalls, M.A., Aasly, J.O., Aharon-Peretz, J., Annesi, G., Barbosa, E.R., Bar-Shira, A., Berg, D., Bras, J., Brice, A., et al. (2009). Multicenter analysis of glucocerebrosidase mutations in Parkinson's disease. N. Engl. J. Med. 361, 1651–1661.

Stryer, L. (1965). The interaction of a naphthalene dye with apomyoglobin and apohemoglobin. A fluorescent probe of non-polar binding sites. J. Mol. Biol. 13, 482–495.

Sun, Y., Quinn, B., Witte, D.P., and Grabowski, G.A. (2005). Gaucher disease mouse models: point mutations at the acid beta-glucosidase locus combined with low-level prosaposin expression lead to disease variants. J. Lipid Res. 46, 2102–2113.

Tayebi, N., Callahan, M., Madike, V., Stubblefield, B.K., Orvisky, E., Krasnewich, D., Fillano, J.J., and Sidransky, E. (2001). Gaucher disease and parkinsonism: a phenotypic and genotypic characterization. Mol. Genet. Metab. 73, 313–321.

Tayebi, N., Walker, J., Stubblefield, B., Orvisky, E., LaMarca, M.E., Wong, K., Rosenbaum, H., Schiffmann, R., Bembi, B., and Sidransky, E. (2003). Gaucher disease with parkinsonian manifestations: does glucocerebrosidase deficiency contribute to a vulnerability to parkinsonism? Mol. Genet. Metab. 79, 104–109.

Thayanidhi, N., Helm, J.R., Nycz, D.C., Bentley, M., Liang, Y., and Hay, J.C. (2010). Alpha-synuclein delays endoplasmic reticulum (ER)-to-Golgi transport in mammalian cells by antagonizing ER/Golgi SNAREs. Mol. Biol. Cell 21, 1850–1863.

Trojanowski, J.Q., and Lee, V.M. (2002). Parkinson's disease and related synucleinopathies are a new class of nervous system amyloidoses. Neurotoxicology 23, 457–460.

Tsika, E., Moysidou, M., Guo, J., Cushman, M., Gannon, P., Sandaltzopoulos, R., Giasson, B.I., Krainc, D., Ischiropoulos, H., and Mazzulli, J.R. (2010). Distinct region-specific alpha-synuclein oligomers in A53T transgenic mice: implications for neurodegeneration. J. Neurosci. 30, 3409–3418.

Volles, M.J., and Lansbury, P.T., Jr. (2003). Zeroing in on the pathogenic form of alpha-synuclein and its mechanism of neurotoxicity in Parkinson's disease. Biochemistry 42, 7871–7878.

Wong, K., Sidransky, E., Verma, A., Mixon, T., Sandberg, G.D., Wakefield, L.K., Morrison, A., Lwin, A., Colegial, C., Allman, J.M., et al. (2004). Neuropathology provides clues to the pathophysiology of Gaucher disease. Mol. Genet. Metab. 82, 192–207.

Xu, Y.H., Quinn, B., Witte, D., and Grabowski, G.A. (2003). Viable mouse models of acid beta-glucosidase deficiency: the defect in Gaucher disease. Am. J. Pathol. 163, 2093–2101.

Xu, Y.H., Sun, Y., Ran, H., Quinn, B., Witte, D., and Grabowski, G.A. (2010). Accumulation and distribution of alpha-synuclein and ubiquitin in the CNS of Gaucher disease mouse models. Mol. Genet. Metab. 102, 436–437.

Zala, D., Benchoua, A., Brouillet, E., Perrin, V., Gaillard, M.C., Zurn, A.D., Aebischer, P., and Deglon, N. (2005). Progressive and selective striatal degeneration in primary neuronal cultures using lentiviral vector coding for a mutant huntingtin fragment. Neurobiol. Dis. 20, 785–798.